Available online at www.sciencedirect.com
ScienceDirect
Polyhedron 27 (2008) 465–472
POLYHEDRON
www.elsevier.com/locate/poly

Synthesis, spectroscopic and structural investigation of $Zn(NCS)_2(nicotinamide)_2$ and $[Hg(SCN)_2(nicotinamide)]_n$

Marijana Đaković [a], Zora Popović [a,*], Gerald Giester [b], Maša Rajić-Linarić [c]

[a] *Laboratory of General and Inorganic Chemistry, Department of Chemistry, Faculty of Science, University of Zagreb, Horvatovac 102a, HR-10000 Zagreb, Croatia*
[b] *Institute of Mineralogy and Crystallography, University of Vienna, Althan Strasse 14, A-1090 Vienna, Austria*
[c] *Laboratory for Thermal Analysis, Brodarski Institute, Marine Research and Special Technology, Av. V. Holjevca 20, HR-10000 Zagreb, Croatia*

Received 10 September 2007; accepted 30 September 2007
Available online 11 December 2007

Abstract

Zinc(II) and mercury(II) thiocyanate complexes with nicotinamide, bis(nicotinamide-*N*)-bis(thiocyanato-*N*)zinc(II) (**1**) and *catena*-[nicotinamide-*N*-(μ-thiocyanato-*S*,*N*)(thiocyanato-*S*)mercury(II)] (**2**), have been prepared and characterized by spectroscopic, thermal and X-ray crystallographic methods. The vibrational bands of diagnostic value are compared to the values of the free ligand and the data are in good correlation with the X-ray results. Centrosymmetrical hydrogen bonded dimers are found, $R_2^2(10)$ in **1** and $R_2^2(8)$ in **2**.

Keywords: Zinc and mercury(II) thiocyanate complexes; Nicotinamide; X-ray crystal structure; IR, NMR spectra; TGA/DTA analysis

1. Introduction

Nicotinamide (pyridine-3-carboxamide, niacinamide, commonly known as vitamin B_3) shows important biological activity *e.g.* in the form of a coenzyme called NAD, nicotinamide adenine dinucleotide, it participates in many amino acid and carbohydrate metabolic reactions; it is also a vital compound in the drug industry. Metal complexes of biologically important ligands are sometimes more effective than the free ligand. Due to the relatively high abundance of zinc in living organisms and its participation in a large number of enzymatic reactions, the zinc complexes of nicotinamide are of great interest – especially those of the heteroleptic type [1]. In this context, we have chosen a thiocyanate ion, a well known ambidentate ligand, which is able to form different molecular architectures through its versatile ligation modes [2]. Beside this, it is interesting that thiocyanates have been found in human biofluids, saliva and cerebrospinal fluid, and recently it was established that psychological stress induces them in oral cavities [3–5]. In addition, the nicotinamide molecule can form a variety of molecular associations via hydrogen bonding, and the present work stems from our interest in finding out the predominant factors to form complexes with desired structural properties so as to create functional ones [6]. In this paper we report the preparation, IR and NMR characterization and structure analysis of $Zn(NCS)_2(nicotinamide)_2$ and $[Hg(SCN)_2(nicotinamide)]_n$. The thermal behaviour of the complexes has also been investigated by TG and DTA techniques. The structural features are compared with a congeneric cadmium(II) nicotinamide complex as well as with analogous zinc complexes, $ZnX_2(nicotinamide)_2$ (X = Cl, Br, I).

2. Experimental

2.1. Materials and physical measurements

All reagents were supplied by Aldrich Chemical Co. and were used as received without further purification. The CHNS microanalyses were measured by the Chemical Analytical Service of the Ruđer Bošković Institute, Zagreb.

* Corresponding author. Tel.: +385 1 4606 354.
E-mail address: zpopovic@chem.pmf.hr (Z. Popović).

0277-5387/$ - see front matter © 2007 Elsevier Ltd. All rights reserved.
doi:10.1016/j.poly.2007.09.036

Infrared spectra were obtained from KBr pellets within the range 4000–400 cm^{-1} with a Perkin–Elmer FTIR spectrometer 1600 Series.

The one-dimensional ^1H and ^{13}C NMR spectra were recorded with a Bruker AV 600 spectrometer, operating at 600.133 MHz and 150.971 MHz for the ^1H and ^{13}C nuclei, respectively. Samples were measured in DMSO-d_6 solution and chemical shifts (ppm) are referred to TMS.

The thermal measurements were performed using a simultaneous TGA–DTA analyser (*TA Instruments*, SDT Model 2960). The TGA and DTA curves were obtained by placing the samples of about 6 mg in mass in small open platinum pans, with a heating rate of 10 °C/min and a nitrogen (purity above 99.996%) flow rate of 50 mL/min. All samples were heated from room temperature up to 700 °C. The SDT was calibrated with indium and silver.

2.2. Preparation of the complexes

2.2.1. Preparation of *[Zn(NCS)$_2$(nia)$_2$]* (**1**)

A warm aqueous solution of nicotinamide (nia) (0.24 g, 0.2 mmol in 50 mL of H_2O) was added to an aqueous solution of zinc nitrate hexahydrate (0.30 g, 0.1 mmol in 10 mL of H_2O). Into the resulting solution was then added an aqueous solution of potassium thiocyanate (0.18 g, 0.2 mmol in 10 mL of H_2O). After keeping the mother liquid for few days, white crystals suitable for X-ray diffraction study were obtained. Total yield corresponds to 85% (0.36 g, 0.87 mmol) based on Zn. *Anal.* Calc. for $C_{14}H_{12}ZnN_6O_2S_2$ (**1**): C, 39.49; H, 2.84; N, 19.74; S, 15.06. Found: C, 39.64; H, 2.94; N, 20.03; S, 15.26%. IR data (cm^{-1}, KBr pellets): 3340s, 3283m-s, 3176m, 3053w, 2358vw, 2343vw, 2094vs, 2044m, 1665vs, 1608s, 1593m, 1482w, 1445w, 1428m-s, 1399m-s, 1338w-m, 1239w, 1202m, 1151w, 1129w, 1113w, 1060m, 1032vw, 961vw, 944w, 855w, 832w-m, 796w, 763w, 704m, 668w-m, 657m, 638m, 589m, 540m.

2.2.2. Preparation of *[Hg(SCN)$_2$(nia)]$_2$* (**2**)

In an aqueous solution of mercury(II) nitrate monohydrate (0.68 g, 0.2 mmol in 100 mL of H_2O) containing a few drops of nitric acid (20% by weight), an aqueous solution of potassium thiocyanate (0.36 g, 4 mmol in 10 mL of H_2O) was added. In a few hours a white crystalline product of mercury(II) thiocyanate was obtained. The crystals were filtered off, washed with water and dried. Total yield of 85% (0.54 g, 1.7 mmol).

Afterwards $Hg(SCN)_2$ was dissolved in ethanol (0.32 g, 1 mmol in 100 mL) by gentle heating and into this still warm solution an ethanol solution of nicotinamide (2 mmol in 30 mL) was added. The mixture was refluxed for 1 h. The clear solution was kept for a few days until white crystals of **2** suitable for X-ray diffraction study were obtained. Total yield corresponds to 77% (0.34 g, 0.77 mmol) based on Hg. *Anal.* Calc. for $C_8H_6HgN_4OS_2$ (**2**): C, 21.89; H, 1.38; N, 12.77; S, 14.61. Found: C, 22.03; H, 1.52; N, 12.89; S, 14.83%. IR data (cm^{-1}, KBr pellets): 3852w, 3452s, 3356s, 2112vs, 1671vs, 1601s, 1572m, 1476w, 1422m, 1394m-s, 1200w-m, 1135w, 1045w, 1028w-m, 829w, 785w, 747w-m, 704m, 641m, 513m.

2.3. X-ray structural analysis

The general and crystal data, and summary of intensity data collection and structure refinement for compounds **1** and **2** are given in Table 1.

Data for structure **1** were collected at 200 K on a Nonius KappaCCD diffractometer with a crystal-detector distance of 30 mm. The extraction and correction of the intensity data, absorption correction and the refinement of the unit cell parameters were performed with the program package DENZO-SMN [7].

Data for structure **2** were collected 293 K on an Oxford Diffraction Xcalibur four-circle kappa geometry single-crystal diffractometer with a Sapphire 3 CCD detector, by applying the CRYSALIS software system [8]. The crystal-detector distance was 60 mm. Data reduction, including absorption correction, was done by the CRYSALIS RED application of the CRYSALIS software system [8].

The structures were solved by direct methods implemented in the SHELXS-97 program [9]. The coordinates and the anisotropic thermal parameters for all non-

Table 1
Crystal data and structure refinement for complexes **1** and **2**

Complex	**1**	**2**
Empirical formula	$C_{14}H_{12}ZnN_6O_2S_2$	$C_8H_6HgN_4OS_2$
Formula weight	425.83	438.90
Temperature (K)	200	296
Wavelength (Å)	0.71073	0.71073
Crystal system	monoclinic	monoclinic
Space group	$C2/c$	$P2_1/c$
a (Å)	18.254(2)	15.1425(7)
b (Å)	4.786(1)	5.8701(3)
c (Å)	21.363(3)	13.5242(7)
β (°)	109.65(1)	96.122(4)
Volume (Å^3)	1757.7(5)	1195.3(1)
Z	4	4
ρ_{calc} (g/cm^3)	1.609	2.439
$F(000)$	864	808
Crystal size (mm)	0.20 × 0.22 × 0.25	0.14 × 0.45 × 0.55
Reflections collected	4825	32416
Unique reflections	2557	3487
Parameters	123	154
$R_{1,\text{all data}}$, R_1^a [$I > 2\sigma(I)$]	0.0275; 0.0238	0.0366; 0.0345
$wR_{2,\text{all data}}$, wR_2^b [$I > 2\sigma(I)$]	0.0650; 0.0632	0.0652; 0.0430
g_1, g_2 in w^c	0.033, 1.0224	0.0204, 2.3946
S^d on F^2	1.061	1.176
$\Delta\sigma_{min/max}$ (e Å^{-3})^e	−0.363/0.463	−1.157/1.025
Extinction coefficient	0.0016(4)	0.0010(2)

[a] $R = \sum ||F_o| - |F_c|| / \sum |F_o|$.

[b] $wR = \left[\sum (F_o^2 - F_c^2)^2 / \sum w(F_o^2)^2\right]^{1/2}$.

[c] $w = 1/\left[\sigma^2(F_o^2) + (g_1P)^2 + g_2P\right]$ where $P = (F_o^2 + 2F_c^2)/3$.

[d] $S = \sum \left[w(F_o^2 - F_c^2)^2 / (N_{obs} - N_{param})\right]^{1/2}$.

[e] The maximum electron density in the last difference Fourier map for **2** is near Hg.

hydrogen atoms were refined by the least-squares method based on F^2 using the SHELXL-97 program [10]. The hydrogen atoms were generated geometrically using the riding model with the isotropic factor set at 1.2 U_{eq} of the parent atom. Hydrogen atoms on carboxamide nitrogen atoms were located in the difference Fourier map at the final stage of the refinement and were refined freely. Graphical work has been performed by the program ORTEP-3 *for Windows* [11] and Mercury 1.4.1 [12]. Thermal ellipsoids are drawn at the 50% probability level.

3. Results and discussion

3.1. Preparation of the complexes

The zinc thiocyanato complex was prepared *in situ* from aqueous solutions by reacting of all the components at room temperature. The mercury complex could not be obtained in the analogous way due to the very low solubility of mercuric thiocyanate in water. By addition of an ethanol solution under *in situ* conditions a mixture of products was obtained instead. But by refluxing the mixture of ethanol solutions of mercuric thiocyanate and nicotinamide, one can prepare the pure titled mercury compound.

3.2. Structure descriptions

All crystals were grown by slow evaporation of the reaction mixture under ambient conditions in a period of two days to one week. Selected bond distances, bond angles and hydrogen bonds are presented in Table 2. The structures are shown in Figs. 1 and 2.

3.2.1. Crystal structure of $Zn(NCS)_2(nia)_2$ (1)

In the molecular structure of bis(nicotinamide-*N*)-bis(thiocyanato-*N*)zinc(II), the zinc atom is located on a center of symmetry and is four coordinated by *N*-atoms from two nicotinamide and two isothiocyanate ligands, as shown in Fig. 1a. The coordination sphere around the central ion is distorted tetrahedral. The angles that deviate the most from regularity are N2–Zn1–N2[1] and N1–Zn1–N1[1] (symmetry code: (1) $-x$, y, $-z+3/2$), closed by two nia and two NCS^- ligands, 112.42(6)° and 123.82(8)°, respectively. Comparing the aforementioned angles in the title compound with the corresponding ones in the analogous tetrahedral zinc(II) halide complex [$ZnX_2(nia)_2$, X = Cl, Br, I] [13–15], compound **1** shows the greatest deviation from an ideal tetrahedral geometry (see Table 3). The largest deviation from ideal tetrahedral angles in all three reported structures occurs for the angles between the same ligands, ∠(X–Zn–X) and ∠(N–Zn–N)py, and this deviation is inversely proportional to the size of the coordinating atom; a small digression in the structure of the bromine complex was observed, Table 3. The Zn–N1/N1[1] (symmetry code: (1) $-x$, y, $-z+3/2$) bond distance (1.928(1) Å) is in the range for reported Zn–N(NCS) bonds in tetrahedral zinc(II) thiocyanate complexes with *m*-substituted pyridine ligands [16–18]. All other bond lengths and angles follow the usual values [19]. The NCS^- groups are almost linear with a N–C–S angle of 177.9(1)° and are coordinated to the zinc ion in a linear fashion with a Zn–N–C angle of 178.8(1)°. The pyridine rings are essentially planar (with a maximum deviation from the mean plane of 0.020(1)Å for the N atom) and the carboxamide group has a dihedral angle of 39.37(7)° with the pyridine plane, Table 4.

Table 2
Selected bond distances (Å) and angles (°) for complexes **1** and **2**

Complex ***1***			
Zn(1)–N(1)	1.928(2)	N(1)–C(1)	1.160(2)
Zn(1)–N(2)	2.033(1)	C(1)–S(1)	1.613(1)
		C(7)–O(1)	1.232(2)
N(1)–Zn(1)–N(1)[1]	123.82(8)	N(1)[1]–Zn(1)–N(2)[1]	104.96(5)
N(2)–Zn(1)–N(1)[1]	105.40(5)	N(1)–Zn(1)–N(2)[1]	105.40(5)
N(1)–Zn(1)–N(2)	104.96(5)	N(2)–Zn(1)–N(2)[1]	112.42(6)
Zn(1)–N(1)–C(1)	178.8(1)		
N(1)–C(1)–S(1)	177.9(1)		
Complex ***2***			
Hg(1)–S(1)	2.459(1)	N(1)–C(1)[2]	1.143(5)
Hg(1)–S(2)	2.419(1)	N(2)–C(2)	1.141(7)
Hg(1)–N(1)	2.387(4)	C(1)–S(1)	1.659(4)
Hg(1)–N(3)	2.333(3)	C(2)–S(2)	1.658(5)
		C(8)–O(1)	1.223(5)
N(1)–Hg(1)–N(3)	91.0(2)	N(3)–Hg(1)–S(1)	104.4(1)
S(1)–Hg(1)–S(2)	128.74(4)	N(3)–Hg(1)–S(2)	116.5(1)
N(1)–Hg(1)–S(1)	106.3(1)	Hg(1)–S(1)–C(1)	94.3(2)
N(1)–Hg(1)–S(2)	102.7(1)	Hg(1)–S(2)–C(2)	98.2(2)

[1] $-x$, y, $-z+3/2$.
[2] x, $y+1$, z.

Fig. 2b shows the crystal packing of **1**, viewed down the *b* axis. In the crystal structure three types of hydrogen bonds, N–H···O, N–H···S and C–H···O, are established. The geometrical parameters are given in Table 5. The centrosymmetric head-to-head hydrogen bond of $R_2^2(8)$ type, usually found in amide structures, is not established in the crystal structure of complex **1**. The carboxamide oxygen atom O(1) participates in a centrosymmetric hydrogen bond of the $R_2^2(10)$ type [20], Scheme 1, with the C4 atom from a pyridine ring of the adjacent molecule [C–H···O, 3.397(2) Å; symmetry code: $1-x$, $2-y$, $-z$]. The oxygen atom is a bifurcated acceptor and it simultaneously accepts an amide hydrogen atom of the neighbouring molecule down the *b* axis [N–H···O, 2.895(2) Å; symmetry code: x, $-1+y$, z] thus forming C(4) hydrogen bond chains in the [0 1 0] direction. The short S···S contacts, very often present in thiocyanate structures [21,22], were not found in the crystal structure of **1**. The sulfur atom from the thiocyanate ligand participates in a N–H···S hydrogen bond with the amide nitrogen [N–H···S, 3.526(2) Å; symmetry code: $1/2-x$, $1/2-y$, $-z$]. Very short Zn···Cg contacts (3.886 Å) between the zinc atom and the pyridine ring of a neighbouring complex molecule located in the direction of the *b* axis are found. Similar short contacts between the metal ion and the aromatic ring have been observed in the crystal structures of aromatic amino acids complexes [23].

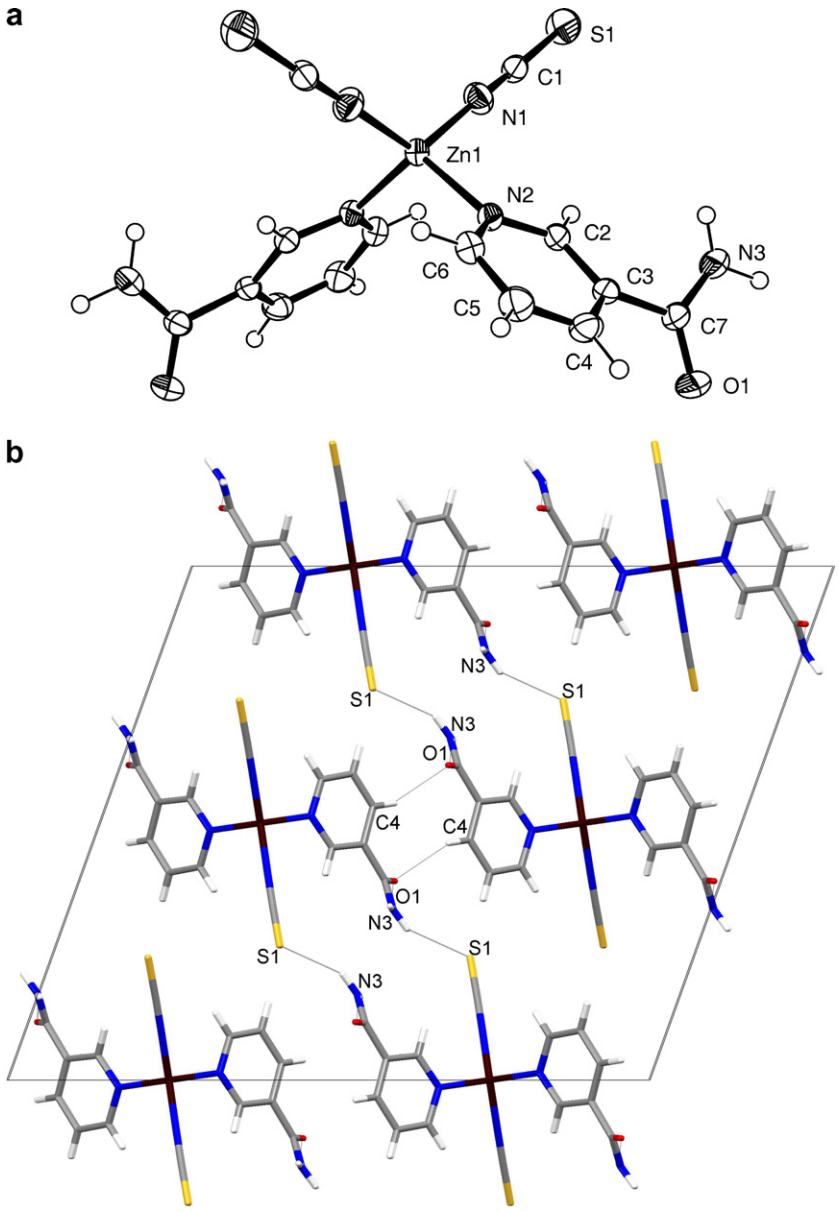

Fig. 1. (a) The ORTEP-3 drawing of the structural unit of complex **1** with the atomic numbering scheme; (b) crystal packing of complex **1** viewed down the *b* axis; hydrogen bonds are represented by dotted lines.

3.2.2. Crystal structure of $[Hg(SCN)_2(nia)]_n$ (**2**)

The X-ray structure analysis of **2** revealed the formation of a single-stranded chain structure, as is displayed in Fig. 2a. Each mercury(II) atom is four coordinated by two bridging μ-SCN-*S*,*N*, one terminal thiocyanate and one nicotinamide ligand in a quite distorted tetrahedral S_2N_2 geometry (the bond angles around the mercury atom are in the range 91.0(2)° to 128.74(4)°, Table 2). The Hg–N as well as the Hg–S bond distances are in the range of those distances found in other Hg^{II} thiocyanate complexes of substituted pyridine-*N* ligands [24–28]. As is expected, both bridging bond distances of coordinated thiocyanate ligands, Hg–N1 [2.387(4) Å] and Hg–S1 [2.459(1) Å] are somewhat longer than those ones of terminal ligands [Hg–N3 2.333(3) Å and Hg–S2 2.419(1) Å]. In **2**, the pyridine ring is less deformed in comparison with **1**, Table 4, and the dihedral angle closed by the pyridine ring and the carboxamide group is also much smaller in **2** than in **1**. Both thiocyanate ligands, bridging and terminal, are coordinated to mercury in a non-linear fashion [∠Hg1–S1–C1 94.3(2)°; ∠Hg1–S2–C2 98.2(2)°], especially the terminal one; its coordination geometry is probably caused by formation of hydrogen bonds. The terminal thiocyanate nitrogen atom is a very common H-bond acceptor and usually participates in more than one hydrogen bonding interaction [22]. In **2** it is a trifurcated acceptor. It participates in two *intra*molecular N–H···N and C–H···N hydrogen bonds of S(10) and S(7) type, respectively, and one *inter*molecular C–H···N hydrogen bond, forming C(7) chains.

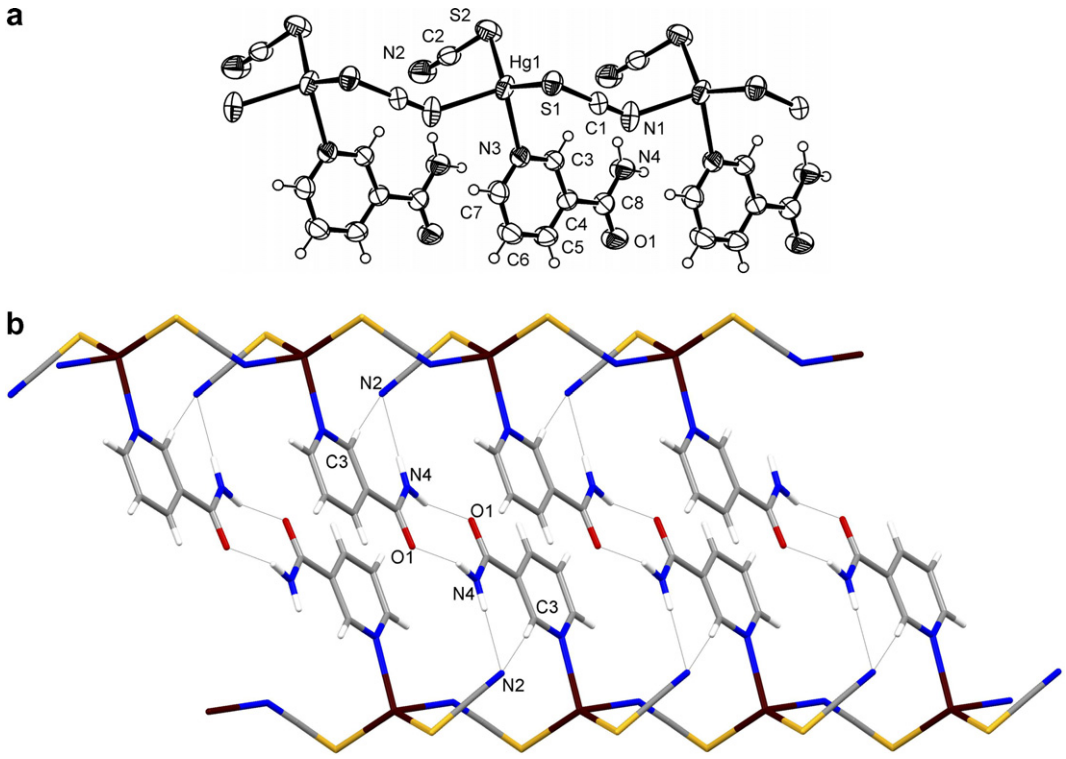

Fig. 2. (a) The ORTEP-3 drawing with the atom-labelling scheme of the structural unit of complex **2**; (b) packing diagram of **2** showing the formation of double-chains by head-to-head double hydrogen bonds of the $R_2^2(8)$ type; hydrogen bonds are represented by dotted lines.

Table 3
Comparison of angles closed by the same ligands in the coordination sphere of complex **1** and analogous halide complexes with nicotinamide [13–15]

	∠(X–Zn–X) (°)	∠(N–Zn–N)py (°)	Zn–N(py) (Å)	CSDB
$Zn(NCS)_2(nia)_2$	123.82(6)	112.42(4)	2.033(1)	
$ZnCl_2(nia)_2$	121.81(5)	101.8(1)	2.058(3)	WUKZAD [13]
			2.057(4)	
$ZnBr_2(nia)_2$	118.9*	96.1*	2.065(3)	BANDUQ [14]
$ZnI_2(nia)_2$	114.72(5)	98.8(1)	2.059(2)	WEMROW [15]

* Deviations are not given by the authors.

Table 4
Selected torsion and dihedral angles (°)

	(**1**)	(**2**)
Py ring (I)	2.16(8)	0.5(3)
Py ring (I) – amido group (I)	39.37(7)	3.0(3)

The details of the hydrogen bonding geometry of **2** are shown in Fig. 2b and geometric parameters are included in Table 4. As shown in Fig. 2b, the polymeric chains are further linked through centrosymmetrical amide–amide hydrogen bonds of the $R_2^2(8)$ type [N···O 2.922(6) Å; symmetry code: $1-x, -y, 1-z$] and in such a way double-chains are formed. These double-chains are packed into a 3D network by the above mentioned C–H···N H–bond in the *c* axis direction. Short C···S contacts [C···S 3.455 Å] are also observed in the structure of **2** between two parallel thiocyanate chains. *Intra* chain pyridine rings, although coplanar, are apart from each other, and no π–π stacking interactions are found.

3.3. Spectroscopic properties

3.3.1. IR spectra

There are two possibilities for nicotinamide to coordinate to a central metal atom, either through the endocyclic nitrogen or the carboxamide oxygen atom. In its Zn and Hg complexes it usually behaves as a monodentate ligand through the pyridine ring nitrogen atom. The coordination mode of the nia ligand could easily be deduced from IR spectra by comparing the IR spectra of the free ligand and the complex molecule. The absorption bands of the carbonyl group (1697, 1679 cm^{-1}) are shifted to lower values if the amide oxygen atom is involved in coordination. In the case of coordination through the pyridine ring nitrogen atom, a significant negative shift of the carbonyl absorption bands takes place [15].

The IR bands of complexes **1** and **2** were assigned by comparing with the free ligand data. In both complexes a shift to lower wavenumbers of *ν*(CO) is observed (1665 cm^{-1} in **1**; 1671 cm^{-1} in **2**). It could be concluded that nia-*O* coordination occurred. Concerning the facts (a) that the CO stretching of picolinamide (pia) in

Table 5
Hydrogen bonds (Å and °) for compounds **1** and **2**

D–H···A	D–H	H···A	D···A	∠DHA	Symmetry code
Compound ***1***					
N(3)–H(23N)···O(1)	0.84(2)	2.08(2)	2.895(2)	163(2)	$x, -1+y, z$
N(3)–H(13N)···S(1)	0.85(2)	2.76(2)	3.526(2)	151(2)	$1/2-x, 1/2-y, -z$
C(4)–H(4)···O(1)	0.95	2.52	3.397(2)	153	$1-x, 2-y, -z$
Compound ***2***					
N(4)–H(14N)···O(1)	0.89(6)	2.03(6)	2.922(6)	175(6)	$1-x, -y, 1-z$
N(4)–H(24N)···N(2)	0.88(7)	2.20(6)	3.064(8)	170(7)	$x, -1+y, z$
C(3)–H(3)···N(2)	0.93	2.44	3.317(8)	135	$x, 5/2-y, -1/2-z$
C(7)–H(7)···N(2)	0.93	2.59	3.370(7)	176	$-1/2+x, 1/2-y, z$

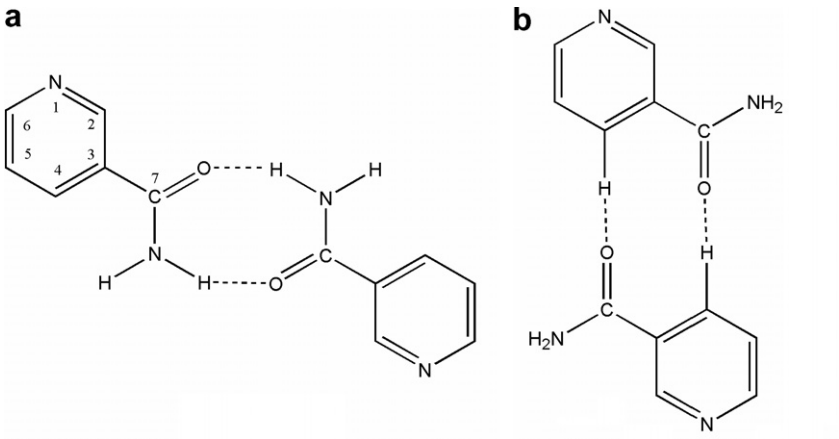

Scheme 1. The bridging modes of nicotinamide established in complexes (a) **1** and (b) **2** with the labelling mode used in the discussion of the NMR data.

acetonitrile solution occurs at 1690 cm^{-1} while it is observed at around 1660 cm^{-1} in solid pia and its complexes [15] where such a negative shift is attributed to hydrogen bonding in the solids, and (b) that halide Zn complexes with nia, as well as Hg complexes with py ligands, are *N*-coordinated, it can be concluded that it could also be the case here, which is confirmed by the X-ray results. Moreover, a greater shift to lower frequencies observed in **1** compared to **2** could be explained by the fact that the carbonyl oxygen atom in **1** participates in two H-bonds as a bifurcated acceptor and significant elongation of C=O bond occurs in comparison to **2** where the carboxamide *O*-atom participates in one H-bond [C–O: 1.232(2) Å in **1**, 1.223(5) Å in **2**].

The *ν*(NH) absorption bands of the amide group in nia appear at 3368 and 3161 cm^{-1}. In both complexes some positive shifts of NH bands occur, and in **1** they are split, while in **2** they are broadened. These shifts to higher frequencies are obviously the consequence of hydrogen bonding in the crystalline state of the complexes. The broadening in **2** could be attributed to three hydrogen bonds in which the amide N-atom is involved as a trifurcated acceptor.

Concerning the C–N stretching frequencies of thiocyanates in general, *ν*(CN) are lower in *N*-bonded complexes (near or below 2050 cm^{-1}) than *S*-bonded complexes (near 2100 cm^{-1}). For bridging complexes (M–SCN–M) the CN stretching frequency is above 2100 cm^{-1} [29]. The stretching CN frequencies of compounds **1** and **2** were observed at 2094 and 2112 cm^{-1}, from which it could be clearly seen that the thiocyanate is coordinated to zinc through the nitrogen atom and to mercury through the sulfur atom. No separate bands were observed for bridging and terminal thiocyanate groups in the mercury complex **2**.

The position of the C–S stretching frequencies in the region 860–690 cm^{-1} is usually employed for differentiating *S*- from *N*-bonded terminal thiocyanates; *ν*(CS) in the range 860–780 cm^{-1} and 720–690 cm^{-1} for *N*- and *S*-coordinated, respectively [30]. However, the *ν*(CS) modes are, for both compounds **1** and **2**, overlapped by pyridine ligand stretching and deformation bands, making the assignment of the C–S stretches quite uncertain.

3.3.2. NMR spectra

The ^{1}H and ^{13}C data for **1** and **2**, together with the literature values of the parent nicotinamide molecule, are presented in Tables 6 and 7, respectively. Scheme 1 shows the labelling of the atoms. The ^{1}H and ^{13}C NMR data of free nia are cited from the literature [31], while the other measurements are performed in DMSO-d_6 solutions. The complexation ^{1}H and ^{13}C NMR shifts are defined as the difference of the proton and carbon shifts, respectively, in the complexes and the free ligand molecule.

Table 6
^{1}H NMR chemical shifts (δ ppm^{-1})[a], complexation shifts ($\Delta\delta$ ppm^{-1})[b,d] and H–H coupling constants (J_{HH}/Hz)[e] in the ligand molecule, nicotinamide, and their complexes with zinc(II) and mercury(II) thiocyanate, **1** and **2**

Compound		nia[c]	**1**	**2**
H-2	δ	9.08	9.04	9.06
	J_{HH}	(s)	(s)	(s)
	$\Delta\delta$		−0.04	−0.02
H-4	δ	8.25	8.24	8.29
	J_{HH}	7.9 (d)	7.94 (d)	7.96 (d)
	$\Delta\delta$		−0.01	0.04
H-5	δ	7.53	7.53	7.59
	J_{HH}	7.9 (d)	7.89 (d)	7.92 (d)
	$\Delta\delta$	4.9 (d)	4.88 (d)	4.96 (d)
			0.00	0.06
H-6	δ	8.74	8.76	8.73
	J_{HH}	4.9 (d)	4.81 (d)	4.76 (d)
	$\Delta\delta$		0.02	−0.01
H-1(NH_2)	δ	7.67	7.62	7.66
	J_{HH}	broadened	broadened	broadened
	$\Delta\delta$		−0.05	−0.01
H-2(NH_2)	δ	8.22	8.18	8.21
	J_{HH}	broadened	broadened	broadened
	$\Delta\delta$		−0.04	−0.01

[a] Referred to TMS in DMSO solutions.
[b] Complexation shifts are defined as the difference of proton chemical shifts between the complex and parent molecule.
[c] Taken from Ref. [31].
[d] Sign (+) denotes deshielding effect, while (−) denotes shielding effect.
[e] Digital resolution ±0.30 Hz: (s) singlet, (d) doublet.

Table 7
^{13}C NMR chemical shifts (δ ppm^{-1})[a] and complexation shifts ($\Delta\delta$ ppm^{-1})[b,d] in the ligand molecule, nicotinamide, and their complexes with zinc(II) and mercury(II) thiocyanate, **1** and **2**

Compound		nia[c]	**1**	**2**
C-2	δ	151.78	151.84	151.85
	$\Delta\delta$		0.06	0.07
C-3	δ	129.70	129.79	130.05
	$\Delta\delta$		0.09	0.35
C-4	δ	135.07	135.39	135.91
	$\Delta\delta$		0.32	0.84
C-5	δ	123.29	123.54	123.82
	$\Delta\delta$		0.25	0.53
C-6	δ	148.65	148.71	148.93
	$\Delta\delta$		0.06	0.28
C-7	δ	166.49	166.43	166.19
	$\Delta\delta$		−0.06	−0.30
C(SCN)	δ		135.05	116.07
	$\Delta\delta$			

[a] Referred to TMS in DMSO solutions.
[b] Complexation shift is defined as the difference of carbon chemical shifts in the complex and the parent molecule.
[c] Taken from Ref. [31].
[d] Sign (+) denotes deshielding effect, while (−) denotes shielding effect.

The ^{1}H spectra of both complexes display six signals, four belonging to aromatic protons and two to carboxamide ones. The signals of the amido group protons as well as the aromatic H–2 proton are found to be shielded in both complexes **1** and **2**.

In the ^{13}C spectra of both complexes **1** and **2**, all the aromatic carbon atoms are shifted 0.06–0.84 ppm downfield relatively to the corresponding ones in the parent ligand molecule. On the basis of the ^{13}C spectra it could be concluded that the aromaticity of the pyridine ring is preserved upon complexation, which can be supported by the short ring C–C distances obtained from the X-ray analysis. The greatest change of ^{13}C chemical shift upon complexation was found at C-4 which is *para* to the nitrogen and *ortho* to the amide group. The complexation shifts of the aromatic carbon atoms are found to be more pronounced by on average 2–3 times more in the mercury complex **2** than in the zinc complex **1**, except for carbon C-2 where the differences in complexation shift are negligible. The carboxamide carbons in **1** and **2** are found to be shielded and the shielding is more pronounced in **2**. In the crystal structure of **1**, the carboxamide oxygen atom participates in two H-bonds as a bifurcated acceptor. This elongates the carbonyl bond and withdraws electron density towards the O-atom more than just one hydrogen bond in which the carboxamide oxygen atom of **2** participates, so the shielding complexation effect is smaller in **1** than in **2**. The hydrogen bonds of the carboxamide groups found in the crystal structure probably also exist in solution.

The formation of thiocyanate and isothiocyanate complexes can be easily detected by the characteristic ^{13}C signal for the -SCN and -NCS groups that are usually found at ~111 and ~145 ppm, respectively [32]. In the ^{13}C spectra of the investigated thiocyanate complexes there are signals at 135 and 116 in the zinc and mercury complex, respectively, indicating the coordination of the thiocyanate ligands to the metal centers through (SCN)-*N* in **1** and through the (SCN)-*S* atom in **2**.

3.4. Thermal analysis

The analysis of the TGA and DTA curves showed that the thermal decomposition of **1** consists of three steps. The first one is the decomposition of **1** to $Zn(SCN)_2$, which corresponds to an endothermic DTA peak at 232.5(5) °C. In the temperature range 250–400 °C two endothermic peaks (a main large one at 283.6(5) °C and a second small one at 351.7(5) °C) were observed. This can be attributed to the thermal decomposition of $Zn(SCN)_2$, and the final residue is ZnS (about 23%).

The thermal analysis of **2** reveals that the thermal decomposition of the investigated complex involves three major processes; two endothermal and an exothermal one. The first endothermal peak corresponds to the melting process of **2** (minimum at 127.8(5) °C). The second one (exothermal at 218.8(5) °C) is followed and overlapped by a small endothermal peak, presenting degradation of the ligands. The incurred $Hg(SCN)_2$ continues the decomposition followed

by sublimation of HgS, corresponding to the endothermic peak with a maximum at 431.2(5) °C.

4. Conclusion

Zinc(II) and mercury(II) thiocyanato complexes with nicotinamide have been synthesized, the zinc complex by the *in situ* reaction in aqueous solution, while the mercury complex by using the previously isolated mercury(II) thiocyanate complex as the mercury starting reagent. The isolated complexes were investigated by X-ray structural analysis, spectroscopic and thermal methods.

The nicotinamide, with the carboxamide group in the *m*-position to the pyridine nitrogen atom acts as a monodentate-*N* ligand for the zinc(II) and mercury(II) ions, coordinating to the metal ions through the pyridine nitrogen atom and leaving both carboxamide moieties available for participation in hydrogen bond formation. The centrosymmetrical amide–amide hydrogen bonds of the $R_2^2(8)$ type, usually found in the structures of amides, are also established in the mercury(II) complex **2**, but in the zinc(II) complex **1**, the presence of a centrosymmetrical head-to-head hydrogen bond of the $R_2^2(10)$ type was found, comprising the aromatic carbon and carboxamide nitrogen atom, Scheme 1. The thiocyanate ion acts as a *N*-donor ligand for zinc, **1**, and a *S*-/μ-*S*,*N*-donor ligand for the mercury complex, **2**. In the thiocyanate complexes of the group 12 metals, the thiocyanate ligand shows its versatile coordination modes, from almost linear in **1** to almost perpendicular in **2**, and with the M-(SCN) angle intermediate in its congeneric cadmium complex [21]. Moreover, in **1** monomeric zinc–thiocyanate units are formed, in **2** there are one-dimensional mercury–thiocyanate chains, while in the cadmium complexes [21] two-dimensional cadmium–thiocyanate sheets are found.

Acknowledgements

This research was supported by the Ministry of Science, Education and Sport of the Republic of Croatia, Zagreb (Grants Nos. 119-1193079-1332 and 192-1252971-1982).

Appendix A. Supplementary material

CCDC 655345 and 655344 contain the supplementary crystallographic data for **1** and **2**. These data can be obtained free of charge via http://www.ccdc.cam.ac.uk/conts/retrieving.html, or from the Cambridge Crystallographic Data Centre, 12 Union Road, Cambridge CB2 1EZ, UK; fax: (+44) 1223-336-033; or e-mail: deposit@ccdc.cam.ac.uk. Supplementary data associated with this article can be found, in the online version, at doi:10.1016/j.poly.2007.09.036.

References

[1] P. Krogsgaard-Larsen, T. Liljefors, U. Madsen, Textbook of Drug Design and Discovery, third ed., Taylor & Francis, London, 2002, p. 365.
[2] H. Zhang, X. Wang, K. Zhang, B.K. Teo, Coord. Chem. Rev. 183 (1999) 157.
[3] P.B. Paul, M.L. Smith, J. Anal. Toxicol. (2006) 511.
[4] N. Goi, Y. Hirai, H. Harada, A. Ikari, T. Ono, Y. Terashima, N. Kinae, M. Hiramatsu, K. Nakamura, H. Tsuboi, K. Takagi, Abstr., Brain, Behav. Immun. 20 (2006) e17.
[5] M. Rosin, T. Kocher, A. Kramer, J. Clin. Periodontol. 28 (2001) 270.
[6] E. Akalin, S. Akyuz, Vib. Spectrosc. 42 (2006) 333.
[7] Z. Otwinowski, W. Minor, in: C.W. Carter, R.M. Sweet (Eds.), Methods in Enzymology, Macromolecular Crystallography, Part A, vol. 276, Academic Press, London, 1997, p. 307.
[8] Oxford Diffraction. Oxford Diffraction Ltd., Xcalibur CCD System, CRYSALIS Software System, Version 171.26, 2004.
[9] G.M. Sheldrick, SHELXS-97, Program for the Automatic Solution of Crystal Structures, University of Göttingen, Germany, 1997.
[10] G.M. Sheldrick, SHELXL-97, Program for the Refinement of Crystal Structures, University of Göttingen, Germany, 1997.
[11] L.J. Farrugia, J. Appl. Crystallogr. 30 (1997) 565.
[12] I.J. Bruno, J.C. Cole, P.R. Edgington, M.K. Kessler, C.F. Macrae, P. McCabe, J. Pearson, R. Taylor, Acta Crystallogr. B 58 (2002) 389.
[13] S. Ide, A. Ataç, Ş. Yurdakul, J. Mol. Struct. 605 (2002) 103.
[14] E. Şahin, S. Ide, A. Ataç, Ş. Yurdakul, J. Mol. Struct. 616 (2002) 253.
[15] H. Paşaoglu, S. Güven, Z. Heren, O. Büyükgüngör, J. Mol. Struct. 794 (2006) 270.
[16] W.-L. Pan, X.-L. Niu, W. Tang, C.-W. Hu, Acta Crystallogr. E 63 (2007) m304.
[17] S. Chantrapromma, H.-K. Fun, X.-J. Feng, J.-X. Yang, J.-Y. Wu, Y.-P. Tian, Acta Crystallogr. E 61 (2005) m733.
[18] F. Bigoli, A. Braibanti, M.A. Pellinghelli, A. Tiripicchio, Acta Crystallogr. B 29 (1973) 2708.
[19] F.H. Allen, O. Kennard, D.G. Brammer, L. Orpen, R. Taylor, J. Chem. Soc., Perkin Trans. 2 (1987) S1.
[20] J. Bernstein, R.E. Davis, L. Shimoni, N.-L. Chang, Angew. Chem., Int. Ed. Engl. 34 (1995) 1555.
[21] G. Yang, H.G. Zhu, B.H. Liang, X.M. Chen, J. Chem. Soc., Dalton Trans. (2001) 580.
[22] M. Đaković, Z. Popović, G. Giester, M. Rajić-Linarić, Polyhedron, in press, doi:10.1016/j.poly.2007.09.014.
[23] K. Aoki, H. Yamazaki, J. Chem. Soc., Dalton Trans. (1987) 2017.
[24] H.-P. Zhou, Y.-P. Tian, J.-Y. Wu, J.-Z. Zhang, D.-M. Li, Y.-M. Zhu, Z.-J. Hu, X.-T. Tao, M.-H. Jiang, Y. Xie, Eur. J. Inorg. Chem. (2005) 4976.
[25] A. Morsali, A. Ramazani, A.R. Mahjuob, A.A. Soudi, Z. Anorg. Allg. Chem. 629 (2003) 2058.
[26] A. Morsali, L.-G. Zhu, Helv. Chim. Acta 89 (2006) 81.
[27] A.R. Mahjoub, A. Morsali, R.E. Nejad, Z. Naturforsch. 59b (2004) 1109.
[28] A. Morsali, A.R. Mahjoub, A. Ramazani, J. Coord. Chem. 57 (1994) 347.
[29] R. Bala, R.P. Sarma, R. Sarma, B.M. Kariuki, Inorg. Chem. Commun. 9 (2006) 852.
[30] R. Kapoor, A. Kataria, A. Pathak, P. Venugopalan, G. Hundal, P. Kapoor, Polyhedron 24 (2005) 1221.
[31] SDBSWeb: http://www.aist.go.jp/RIODB/SDBS/ (National Institute of Advanced Industrial Science and Technology, 18.01.2007).
[32] N. Iranpoor, H. Firouzabadi, H.R. Shaterian, Tetrahedron Lett. 43 (2002) 3439.